

Supplementary information S1 | **Genome-wide RNA-structure probing technologies****Probing of RNA G-quadruplex structures *in vitro* and *in vivo***

With a mostly repressive role in translation suggested for mRNA RG4 structures when assessed *in vitro*, the physiological relevance of the RG4 structure inside cells becomes a critical question. Indeed, beside their role in several proto-oncogene mRNAs associated with eIF4A hyperactivation and cancer development<sup>1</sup>, 5' UTR RG4 structures have been functionally implicated in neurodegenerative diseases<sup>2</sup> (reviewed in ref.<sup>3</sup>) and in local translation in neurons (reviewed in ref.<sup>4</sup>). Moreover, almost 10,000 human 5' UTRs are estimated to contain at least one RG4 sequence by bioinformatics prediction<sup>5</sup>. (Note that the enrichment for RG4s is not limited to the 5' UTR, but includes the CDS and 3' UTR<sup>6,7</sup>.) However, it has been challenging to detect RG4s in mRNAs inside cells to confirm their relevance. Classically, RG4 structures have been assessed by biophysical methods *in vitro*, such as circular dichroism (CD) spectroscopy<sup>8</sup> — a typical CD signature of a parallel RG4 structure is a positive peak at 265 nm and a negative peak at 240 nm, expressed as its 'molar ellipticity'; UV thermal melting<sup>9</sup> — a thermal difference spectrum is obtained by recording the UV absorbance spectra of the unfolded and folded states of an RNA structure at above and below melting temperature, which yields a spectrum unique to the RG4 structure; or NMR spectroscopy<sup>10</sup> (see the figure). For example, CD spectroscopy was used to assess the RG4 structures of RNA oligomers of the eIF4A-dependent 5' UTR motifs<sup>1</sup>, which have been compared to an accepted telomere DNA G-quadruplex structure<sup>11</sup>. These methods report RG4 structural features in isolation and without flanking RNA sequence. RG4s embedded in mRNA sequence have been addressed by in-line probing *in vitro*<sup>12,13</sup>. New approaches use RG4-specific antibodies or stabilizing ligands to visualize RG4 structures in human cells<sup>14</sup>, or compare RNase footprints on RNA and 7-deazaguanine RNA unable to fold into RG4s, to confirm RG4 formation in longer RNAs *in vitro*<sup>15</sup>. Importantly, RG4 structures can be stabilized by cations, especially by potassium (K<sup>+</sup>), while lithium ions (Li<sup>+</sup>) do not favor RG4 formation. A genome-wide *in vitro* approach exploits the interaction of RG4s with cations and ligands to induce reverse transcription (RT) stalling<sup>16</sup>, termed rG4-seq<sup>17</sup>. This method indicated that RG4s are formed in human telomerase RNA, for example, in RNA extracted from HeLa cells<sup>16</sup>, and globally mapped thousands of RG4s *in vitro*<sup>17</sup>. To improve nucleotide resolution, selective 2'-hydroxyl acylation analyzed by primer extension (SHAPE) was combined with Li<sup>+</sup>-based primer extension (LiPE), termed SHALiPE, to map RG4s *in vitro*<sup>18</sup>. This method makes use of Li<sup>+</sup> and K<sup>+</sup> in their ability to disfavor and favor RG4 folding, respectively.

Despite the extensive methods developed for RG4 structures *in vitro*, convincing confirmation of RG4 formation inside living cells has been lacking. SHAPE- and dimethyl sulfate (DMS)-based RNA structure probing protocols do not give a clear signature for RG4 3D folds. However, RG4 structures block RT reactions in a K<sup>+</sup>-dependent manner and protect the N<sup>7</sup> of a G-nucleotide in a RG4 from DMS-modification. Thus, the combination of DMS treatment before profiling RT stops recently allowed probing RG4s in cells<sup>19</sup>. This study found that >10,000 mammalian and yeast RNA regions can form RG4s *in vitro*, but they were accessible to DMS *in vivo* and therefore each appeared unfolded at significant frequency in cells<sup>19</sup>. Representative RG4s that were unfolded in eukaryotic cells were folded in bacteria where they slowed down growth and translation. This observation suggests that in eukaryotes, RG4s may be actively kept in an unfolded conformation by RNA helicases or single-strand-specific RBPs. However, the observation does not rule out biological relevance of the RG4 at specific stages of an mRNA's existence, for example during nuclear pre-mRNA processing or ribosomal scanning in translation initiation. Thus, it is not clear whether RG4s are folding under physiological conditions in eukaryotic

cells. Indeed, high-resolution NMR or crystal structures of naturally occurring complex RNA folds such as rRNAs, tRNAs, ribozymes or riboswitches have so far not revealed RG4 motifs within these structures. This absence suggests that RG4s are selected against in long-lived structures but leaves open the possibility that they form temporarily and impact gene regulation. Together, RG4 structures illustrate a potentially interesting example of structured RNA elements within 5' UTRs, yet raise the need for new methodologies to probe and assess their relevance *in vivo*.

### Genome-wide *in vitro* RNA structure probing: What is the folding state of the transcriptome?

In recent years, the field of RNA structure probing has developed new approaches that can map RNA secondary structures of the transcriptome *in vitro* using high-throughput sequencing (reviewed in ref.<sup>20</sup>). Multiple studies that probed total RNA extracted from cells folded *in vitro* using RNases, SHAPE or DMS<sup>21–26</sup> have led to different conclusions regarding mRNA folding states. UTRs of mRNAs were found to be generally less structured in yeast<sup>21</sup>, but more structured in mouse cells<sup>25</sup>, compared to coding regions. Interestingly, global RNA structure mapping *in vitro* already detects individual variations in RNA structure across the human population<sup>27,28</sup>. Analysis of a family trio of father, mother and child using *in vitro* probing of native RNA from cells<sup>27</sup>, for example, showed that 15% of all transcribed, mostly heritable single nucleotide variants (SNVs) alter local RNA structure allele-specifically and can contribute to disease<sup>29</sup>. For example, such “riboSNitches” in the 5' UTR can cause SHAPE-probed RNA structure changes in the ferritin light chain (FTL)<sup>30</sup> and retinoblastoma 1 (RB1)<sup>31</sup> mRNAs, associated with hyperferritinaemia cataract syndrome, an early onset of cataract, and retinoblastoma, respectively. The variant found in the ferritin 5' UTR variant is proposed to disrupt an IRE hairpin and abolish IRE-IRP RNP formation<sup>30</sup> and the associated translation regulation. It remains to be determined whether these proposed RNA structure changes occur and dysregulate translation in cells or in patients.

### Global *in vivo* RNA structure probing: Is the transcriptome unfolded inside cells?

Based on methods to probe individual RNA structures *in vivo*<sup>32–35</sup>, three DMS-based methods and an adaptation of SHAPE have been coupled to deep sequencing to globally map RNA structures *in vivo* (reviewed in refs.<sup>36–39</sup>). Sequencing of a cDNA library and mapping of millions of reads of modification or cleavage sites onto the genome provides insight into whether an RNA is structured, linear or flexible — existing in a heterogeneous array of different conformations — at a specific nucleotide position. Two independent methods both use cell-permeable DMS<sup>32</sup>. Structure-seq<sup>40,41</sup> in the plant *Arabidopsis thaliana* yielded structure information for over 10,000 transcripts. A three-nucleotide periodicity at mRNA coding regions, with a high structural periodicity only in highly translated coding regions, and unstructured bases preceding the start codon implies that mRNA structure is linked to translation. Similarly, DMS-seq<sup>24</sup> found that the transcriptome inside yeast and mammalian cells is overall less structured compared to its refolded state *in vitro*. In addition, Mod-seq (modification using high-throughput sequencing) was also applied for DMS in yeast<sup>42</sup> but can be used with any small molecule probe that modifies RNA according to the accessibility of its bases due to structure.

Unlike DMS, which selectively labels unprotected adenine and cytosine for reverse transcription readout<sup>32</sup>, SHAPE marks accessible unpaired bases in all four nucleotides. In *in vivo* click SHAPE (icSHAPE)<sup>43</sup>, an advanced cell-permeable SHAPE probe<sup>44</sup>, 2-methylnicotinic acid imidazolide (NAI)-N<sub>3</sub>, allows *in vivo* RNA labeling and uses click chemistry to attach biotin for purification of modified RNA. icSHAPE was used to compare RNA structures inside embryonic stem cells to *in vitro*-folded purified RNA, and revealed that RNA structures around translation initiation sites and ribosome pause sites are similar *in vitro* and *in vivo* whereas protein binding sites and RNA modification sites in mRNAs show

local changes in RNA structure *in vivo* compared to *in vitro*. Owing to their distinct modification of RNA, DMS- and SHAPE-based methods provide different and complementary structure information and each has their own advantages and challenges.

### **Gains and challenges of genome-wide *in vivo* RNA-structure probing methods**

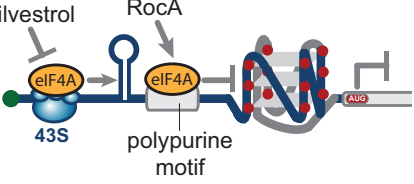
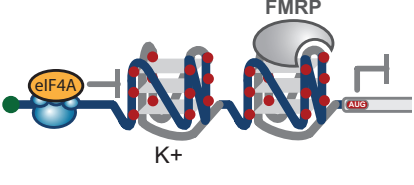
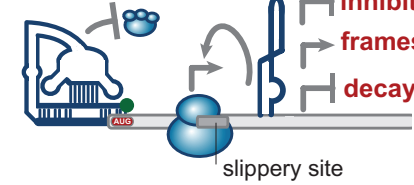
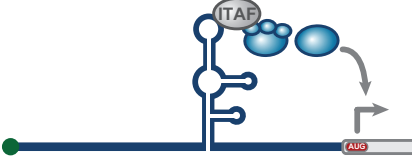
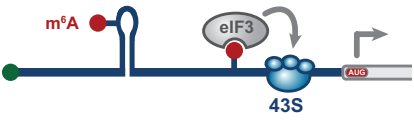

The burst of new technologies to probe RNA structure in living cells may enable a detailed interpretation of the folding state of RNAs in their native environments and illuminate comparisons to their intrinsic ability to fold *in vitro*. However, these different technologies each come with their own sets of pros and cons due to differences in the chemistries of RNA modification, processing of RNA and DNA fragments, and sequence alignment and analysis tools. Technical details have been compared in recent reviews<sup>20,36,37</sup> but issues of structural and biological interpretation are briefly reviewed here. First, structure modeling heavily relies on bioinformatics-assisted or manual prediction to build RNA structure models. However, in terms of modeling specific structures, SHAPE, DMS, and other nucleotide-resolution probing data do not directly identify base pairs as these probes modify RNA according to their nucleotide accessibility, the overall “structured-ness” of RNAs. The availability of these data has not typically increased predictive power for specific base pairs in blind modeling challenges<sup>45</sup>. In addition, due to their nucleotide selectivity, these probes provide different structure information. If the accessibility of an unpaired nucleotide is disguised by protein interaction, its structure profile can look the same as in double-stranded RNA or as if it was not probed. Second, beyond these ambiguities in structural interpretation, probing reagents modify macromolecules and are *per se* toxic to cells. As DMS and SHAPE probing require treatment of cells with the probe for minutes, detected RNA structures may partly represent RNA folding rearrangement upon non-physiological stress and apoptosis conditions. How fast and to what extent RNA structures are remodeled in cells upon probing is largely unknown. Furthermore, these events are expected to be distinct from specific conformational changes, where proteins capture RNAs in different folding states. Third, probing obtains a snapshot as an average over many dynamic RNA structures. In many and perhaps most cases, the functional impact of mRNA structure may not be accurately understood in terms of a defined secondary or tertiary structure. Finally, structure analysis of low abundant mRNAs presents additional caveats due to the typically low signal-to-noise ratio obtained for these molecules in chemical probing. Enriching for SHAPE-modified RNA fragments before sequencing, as in icSHAPE<sup>43</sup>, and amplifying cDNAs for specific target mRNAs, can potentially overcome this problem. Each of these issues is well appreciated in the structure probing field and inspires the further improvement of the RNA structure probing toolbox for *in vivo* use.

### **RNA structure technologies that target RNA–RNA interactions *in vivo***

In addition to RNA structures within one molecule, RNA can also form long-range intermolecular duplexes when two different RNAs interact. These dynamic duplexes are important during many key steps of gene expression. For example, interactions between small nuclear RNAs and pre-mRNAs mediate splicing, base pairing between tRNAs and mRNAs allows decoding by the ribosome, and small RNA interactions with mRNAs repress their translation and stability. Accessibility probing and computational predictions give poor accuracy in modeling complex interactions. Several approaches are being investigated to detect ultraviolet (UV)-crosslinked RNA duplex interaction sites of target RBPs<sup>46–49</sup> (typically in the 3' UTR) and to leverage RNA proximity ligation (RPL) to avoid crosslinking which ligates close interacting RNA contact sites<sup>50</sup>. In addition, three concurrently published protocols use the RNA probe psoralen: Ligation of interacting RNA and high-throughput sequencing (LIGR-seq)<sup>51</sup>, sequencing of psoralen-crosslinked, ligated, and selected hybrids (SPLASH)<sup>52</sup>, and psoralen analysis of

RNA interactions and structures (PARIS)<sup>53</sup>. Psoralen intercalates into RNA-RNA duplexes upon UV-treatment at UpA motifs<sup>54</sup> and can thereby capture complex structures such as pseudoknots. It is worth noting that the required treatment of cells with psoralen and UV for about 5-10 and 20-30 minutes, respectively, sometimes on ice, may have toxic side effects. Sequencing of psoralen-crosslinked duplexes monitors global RNA-RNA sites with near base pair resolution inside cells without the need for knowledge of existing RNA-RNA or RNA-protein interactions. All methods detect long-range structures and RNA-RNA interactions in *cis* and *trans* and report alternative duplex conformations, many of which can occur between RNA regions separated by hundreds or thousands of nucleotides. While LIGR-seq and PARIS are based on the psoralen derivative 4'-aminomethyltrioxalen (AMT), SPLASH uses enrichment of biotinylated-psoralen modified duplexes. SPLASH showed that in human and yeast cells, 5' UTR, CDS and 3' UTR bases preferentially interact with other bases in the same domain and indicates functional structured elements mainly in UTRs. In fact, co-regulated mRNAs were found to base pair with each other. However, these chemical crosslinking approaches have typically produced a significant fraction of RNA-RNA pairings that conflict with RNA structures determined through for example crystallography of ribosome structures<sup>53,55</sup>. In addition, especially for low-abundant mRNAs, validation of these methods is limited by the required ligation efficiency and sequencing depth to detect mRNA-containing duplexes.

Figure | **Probing methods used to assess categories of RNA structures discussed in the Review**

mRNA structure class	RNA structure probing method
<p><b>eIF4A and complex 5'UTRs</b></p>  <p>silvestrol RocA eIF4A eIF4A 43S polypurine motif AUG</p>	<p>circular dichroism (RG4) UV thermal melting (RG4) toeprinting (eIF4A) RNase I footprinting (eIF4A)</p>
<p><b>RNA G-quadruplex</b></p>  <p>eIF4A FMRP K+ AUG</p>	<p>circular dichroism UV thermal melting in-line probing rG4-seq, cation/ligand interactions, RT-stalling SHAPE-seq, SHALiPE-seq DMS-seq FOLDeR footprinting (FMRP)</p>
<p><b>pseudoknot</b></p>  <p>inhibition frameshift decay slippery site AUG</p>	<p>chemical/enzymatic probing nuclease mapping SHAPE in-line probing cryo-EM</p>
<p><b>IRES</b></p>  <p>TAF 43S AUG</p>	<p><u>viral IRES</u> chemical/enzymatic probing SHAPE cryo-EM, NMR, x-ray crystallography <u>cellular IRES</u> chemical/enzymatic probing SHAPE, mutate-and-map MOHCA-seq</p>
<p><b>m<sup>6</sup>A RNA modification</b></p>  <p>m<sup>6</sup>A eIF3 43S AUG</p>	<p>enzymatic probing (m<sup>6</sup>A switch) icSHAPE-seq toeprinting (eIF3) NMR, thermodynamic measurements</p>
<p><b>eIF3-binding stem-loop</b></p>  <p>eIF3 3d AUG</p>	<p>SHAPE</p>

## References:

1. Wolfe, A. L. *et al.* RNA G-quadruplexes cause eIF4A-dependent oncogene translation in cancer. *Nature* **513**, 65–70 (2014).
2. Haeusler, A. R. *et al.* C9orf72 nucleotide repeat structures initiate molecular cascades of disease. *Nature* **507**, 195–200 (2014).
3. Simone, R., Fratta, P., Neidle, S., Parkinson, G. N. & Isaacs, A. M. G-quadruplexes: Emerging roles in neurodegenerative diseases and the non-coding transcriptome. *FEBS Letters* **589**, 1653–1668 (2015).
4. Schofield, J. P. R., Cowan, J. L. & Coldwell, M. J. G-quadruplexes mediate local translation in neurons. *Biochem. Soc. Trans.* **43**, 338–342 (2015).
5. Beaudoin, J. D. & Perreault, J. P. 5'-UTR G-quadruplex structures acting as translational repressors. *Nucleic Acids Res.* **38**, 7022–7036 (2010).
6. Beaudoin, J. D. & Perreault, J. P. Exploring mRNA 3'-UTR G-quadruplexes: Evidence of roles in both alternative polyadenylation and mRNA shortening. *Nucleic Acids Res.* **41**, 5898–5911 (2013).
7. Thandapani, P. *et al.* Aven recognition of RNA G-quadruplexes regulates translation of the mixed lineage leukemia protooncogenes. *Elife* **4**, 1–30 (2015).
8. Paramasivan, S., Rujan, I. & Bolton, P. H. Circular dichroism of quadruplex DNAs: Applications to structure, cation effects and ligand binding. *Methods* **43**, 324–331 (2007).
9. Mergny, J. L., Li, J., Lacroix, L., Amrane, S. & Chaires, J. B. Thermal difference spectra: A specific signature for nucleic acid structures. *Nucleic Acids Res.* **33**, 1–6 (2005).
10. Webba da Silva, M. NMR methods for studying quadruplex nucleic acids. *Methods* **43**, 264–277 (2007).
11. Moye, A. L. *et al.* Telomeric G-quadruplexes are a substrate and site of localization for human telomerase. *Nat. Commun.* **6**, 7643, 1–12 (2015).
12. Regulski, E. E. & Breaker, R. R. In-line probing analysis of riboswitches. *Methods Mol. Biol.* **419**, 53–67 (2008).
13. Beaudoin, J. D., Jodoin, R. & Perreault, J. P. In-line probing of RNA G-quadruplexes. *Methods* **64**, 79–87 (2013).
14. Biffi, G., Di Antonio, M., Tannahill, D. & Balasubramanian, S. Visualization and selective chemical targeting of RNA G-quadruplex structures in the cytoplasm of human cells. *Nat. Chem.* **6**, 75–80 (2013).
15. Weldon, C. *et al.* Identification of G-quadruplexes in long functional RNAs using 7-deazaguanine RNA. *Nat. Chem. Biol.* **13**, 18–20 (2016).
16. Kwok, C. K. & Balasubramanian, S. Targeted detection of G-quadruplexes in cellular RNAs. *Angew. Chemie - Int. Ed.* **54**, 6751–6754 (2015).
17. Kwok, C. K., Marsico, G., Sahakyan, A. B., Chambers, V. S. & Balasubramanian, S. rG4-seq reveals widespread formation of G-quadruplex structures in the human transcriptome. *Nat. Methods* **13**, 841–844 (2016).
18. Kwok, C. K., Sahakyan, A. B. & Balasubramanian, S. Structural analysis using SHALiPE to reveal RNA G-quadruplex formation in human precursor microRNA. *Angew. Chemie - Int. Ed.* **55**, 8958–8961 (2016).
19. Guo, J. U. & Bartel, D. P. RNA G-quadruplexes are globally unfolded in eukaryotic cells and depleted in bacteria. *Science* **353**, aaf5371, 1–8 (2016).
20. Wan, Y., Kertesz, M., Spitale, R. C., Segal, E. & Chang, H. Y. Understanding the transcriptome through RNA structure. *Nat. Rev. Genet.* **12**, 641–655 (2011).
21. Kertesz, M. *et al.* Genome-wide measurement of RNA secondary structure in yeast. *Nature* **467**, 103–107 (2010).
22. Underwood, J. G. *et al.* FragSeq: transcriptome-wide RNA structure probing using high-throughput sequencing. *Nat. Methods* **7**, 995–1001 (2010).
23. Lucks, J. B. *et al.* Multiplexed RNA structure characterization with selective 2'-hydroxyl acylation analyzed by primer extension sequencing (SHAPE-Seq). *Proc. Natl. Acad. Sci. U. S. A.* **108**, 11063–11068 (2011).
24. Rouskin, S., Zubradt, M., Washietl, S., Kellis, M. & Weissman, J. S. Genome-wide probing of RNA structure reveals active unfolding of mRNA structures in vivo. *Nature* **505**, 701–705 (2014).
25. Incarnato, D., Neri, F., Anselmi, F. & Oliviero, S. Genome-wide profiling of mouse RNA secondary structures reveals key features of the mammalian transcriptome. *Genome Biol.* **15**, 491, 1–13 (2014).
26. Siegfried, N. a, Busan, S., Rice, G. M., Nelson, J. a E. & Weeks, K. M. RNA motif discovery by SHAPE and mutational profiling (SHAPE-MaP). *Nat. Methods* **11**, 959–965 (2014).
27. Wan, Y. *et al.* Landscape and variation of RNA secondary structure across the human transcriptome. *Nature* **505**, 706–709 (2014).
28. Corley, M., Solem, A., Qu, K., Chang, H. Y. & Laederach, A. Detecting riboSNitches with RNA folding algorithms: A genome-wide benchmark. *Nucleic Acids Res.* **43**, 1859–1868 (2015).
29. Halvorsen, M., Martin, J. S., Broadaway, S. & Laederach, A. Disease-associated mutations that alter the RNA structural ensemble. *PLoS Genet.* **6**, 1–11 (2010).
30. Martin, J. S. *et al.* Structural effects of linkage disequilibrium on the transcriptome. *RNA* **18**, 77–87 (2012).
31. Kutchko, K. M. *et al.* Multiple conformations are a conserved and regulatory feature of the RB1 5' UTR. *RNA* **21**, 1274–1285 (2015).
32. Wells, S. E., Hughes, J. M. X., Haller Igel, A. & Ares Jr., M. Use of dimethyl sulfate to probe RNA structure in vivo. *Methods Enzymol.* **318**, 479–493 (2000).
33. Wilkinson, K. A. *et al.* High-throughput SHAPE analysis reveals structures in HIV-1 genomic RNA strongly conserved across distinct biological states. *PLoS Biol.* **6**, 883–899 (2008).
34. Liebeg, A. & Waldsich, C. Probing RNA structure within living cells. *Methods Enzymol.* **468**, 219–238 (2009).

35. Zemora, G. & Waldsich, C. RNA folding in living cells. *RNA Biol.* **7**, 634–641 (2010).
36. Kwok, C. K., Tang, Y., Assmann, S. M. & Bevilacqua, P. C. The RNA structurome: Transcriptome-wide structure probing with next-generation sequencing. *Trends Biochem. Sci.* **40**, 221–232 (2015).
37. Kubota, M., Tran, C. & Spitale, R. C. Progress and challenges for chemical probing of RNA structure inside living cells. *Nat. Chem. Biol.* **11**, 933–941 (2015).
38. Bevilacqua, P. C., Ritchey, L. E., Su, Z. & Assmann, S. M. Genome-wide analysis of RNA secondary structure. *Annu. Rev. Genet.* **50**, 235–266 (2016).
39. Incarnato, D. & Oliviero, S. The RNA epistructurome: Uncovering RNA function by studying structure and post-transcriptional modifications. *Trends Biotechnol.* **35**, 318–333 (2017).
40. Ding, Y. *et al.* In vivo genome-wide profiling of RNA secondary structure reveals novel regulatory features. *Nature* **505**, 696–700 (2014).
41. Ritchey, L. E. *et al.* Structure-seq2: sensitive and accurate genome-wide profiling of RNA structure in vivo. *Nucleic Acids Res.* **45**, 1–9 (2017).
42. Talkish, J., May, G., Lin, Y., Jr, J. L. W. & Mcmanus, C. J. Mod-seq: high-throughput sequencing for chemical probing of RNA structure. *RNA* **20**, 713–720 (2014).
43. Spitale, R. C. *et al.* Structural imprints in vivo decode RNA regulatory mechanisms. *Nature* **519**, 486–490 (2015).
44. Spitale, R. C. *et al.* RNA SHAPE analysis in living cells. *Nat. Chem. Biol.* **9**, 18–20 (2013).
45. Miao, Z. *et al.* RNA-Puzzles Round III: 3D RNA structure prediction of five riboswitches and one ribozyme. *RNA* **23**, 655–672 (2017).
46. Gong, C. & Maquat, L. E. lncRNAs transactivate STAU1-mediated mRNA decay by duplexing with 3' UTRs via Alu elements. *Nature* **470**, 284–288 (2011).
47. Kudla, G., Granneman, S., Hahn, D., Beggs, J. D. & Tollervey, D. Cross-linking, ligation, and sequencing of hybrids reveals RNA-RNA interactions in yeast. *Proc. Natl. Acad. Sci. U. S. A.* **108**, 10010–10015 (2011).
48. Grosswendt, S. *et al.* Unambiguous Identification of miRNA: Target site interactions by different types of ligation reactions. *Mol. Cell* **54**, 1042–1054 (2014).
49. Sugimoto, Y. *et al.* hiCLIP reveals the in vivo atlas of mRNA secondary structures recognized by Staufen 1. *Nature* **519**, 491–494 (2015).
50. Ramani, V., Qiu, R. & Shendure, J. High-throughput determination of RNA structure by proximity ligation. *Nat. Biotechnol.* **33**, 980–984 (2015).
51. Sharma, E., Sterne-Weiler, T., O'Hanlon, D. & Blencowe, B. J. Global mapping of human RNA-RNA interactions. *Mol. Cell* **62**, 1–9 (2016).
52. Aw, J. G. A. *et al.* In vivo mapping of eukaryotic RNA interactomes reveals principles of higher-order organization and regulation. *Mol. Cell* **62**, 603–617 (2016).
53. Lu, Z. *et al.* RNA duplex map in living cells reveals higher-order transcriptome structure. *Cell* **165**, 1–13 (2016).
54. Harris, M. E. & Christian, E. L. RNA crosslinking methods. *Methods Enzymol.* **468**, 127–46 (2009).
55. Sergiev, P. V., Dontsova, O. A. & Bogdanov, A. A. Chemical methods for the structural study of the ribosome: Judgment day. *Mol. Biol.* **35**, 472–495 (2001).